JOURNAL OF GEOPHYSICAL RESEARCH, VOL. 103, NO. D19, PAGES 25,397–25,408, OCTOBER 20, 1998

The impact of spatial averaging on calculated polar ozone loss
1. Model experiments

Kate R. Searle,[1] Martyn P. Chipperfield, Slimane Bekki,[2] and John A. Pyle

Centre for Atmospheric Science, University of Cambridge, Cambridge, England, United Kingdom

Abstract. We have used an off-line chemical transport model (CTM) to investigate the effect of model resolution on the calculated ozone destruction in the Arctic lower stratosphere in winter and spring. The CTM was forced using the meteorology of the 1994-1995 winter for horizontal resolutions from $5.6^o \times 5.6^o$ to $1.4^o \times 1.4^o$. Using both a full chemistry scheme and a simple chemistry scheme based only on the ClO-ClO catalytic ozone destruction cycle, we find very little sensitivity of the polar ozone loss to model resolution. This lack of sensitivity is due to the effectively complete activation of chlorine at all model resolutions during this cold winter, which removes any potential effect of spatial averaging on the ClO distribution. Our model results are in strong contradiction with the recent calculations of *Edouard et al.* [1996]. The differences may be due to differences in tracer diffusion between the studies. Comparison of the filamentary structures produced in the ClO_x fields from the simple and full chemistry schemes show that chemistry plays an important role in determining the lifetime of these features in the model. Narrow filaments, which are no longer apparent in the full chemistry integrations, persist for much longer in the simple chemistry case at the same resolution.

1. Introduction

The notion that the finite spatial resolution at which a chemical model is run may produce an effect on the behavior of the model is well known. The origin of the problem lies in the fact that the species concentrations within each model grid box are an average of the true concentrations found within that volume, and it is the neglect of the subgrid-scale structures which can produce a dependency of the model chemistry on the model resolution. Whether the model overestimates or underestimates a rate of reaction will depend upon whether the species involved in the reaction are correlated (model rate < real rate) or anticorrelated (model rate > real rate). The magnitude of the error is also dependent upon the amount of variation present in the fields of the reactants: if either of the reacting species has a constant value within a region, there can be no resolution dependency, if all other factors controlling chemical rates (for example temperature and pressure) are the same. This latter point suggests that there are regions of the atmosphere where resolution is important: predominantly, the midlatitude surf zone, and others, such as the vortex regions where the relatively constant fields, will lead to resolution having only a small impact.

The chemical problems associated with the limited resolution of numerical models have been considered in a number of different contexts by a variety of authors, with initial concern centering on the averaging problems produced through the use of global or zonal averages and averaged temperature fields [*Tuck*, 1979; *Kaye*, 1987; *Pyle and Zavody*, 1990]. Recent efforts have addressed the possible role that averaging and the absence of accurate mixing on a subgrid-scale could be playing in the way in which polar and middle latitude ozone losses are modeled. In particular, *Thuburn and Tan* [1997] and *Tan et al.* [1998] examined the way in which mixing of ClO_x-rich vortex air with middle latitude air might be parameterized and the effects of the neglect of such processes.

Recently, *Edouard et al.* [1996] (hereafter referred to as E96) presented model calculations of the accumulated Arctic ozone loss over the 1994-1995 winter. They used a single-layer, isentropic transport model run at different resolutions on the 450 K surface with a simplified description of ozone loss chemistry based

[1]Now at United Kingdom Meteorological Office, Bracknell, England, United Kingdom.

[2]Now at Service d'Aeronomie du Centre National de la Recherche Scientifique, Université Pierre et Marie Curie, Paris, France.

Paper number 98JD02090.
0148-0227/98/98JD-02090$09.00

on the ClO-ClO catalytic cycle. They found a very strong dependence of the calculated ozone loss within the polar vortex on the model resolution. They attributed it to the non linear dependence of ozone loss rate on active chlorine (ClO_x) concentrations coupled with the neglect of subgrid-scale features at low resolution. E96 noted that the large difference (~40%) in ozone loss by the end of March between their lowest-resolution integration and their highest resolution integration was of similar magnitude to the discrepancy between a low resolution full chemistry model run and the inferred column O_3 depletion based on ground-based Système d'Analyse par Observation Zénithale (SAOZ) observations [*Goutail et al.*, 1998]. From this 40% figure, E96 suggested that the discrepancy between the three-dimensional (3-D) model column results and the measurements could be explained solely by the limited resolution of the 3-D model, leading to the neglect of subgrid-scale features. However, this apparent quantitative agreement of 40% might have been fortuitous. The percentage differences between SAOZ and the 3-D model varied greatly throughout the considered period, peaking at a maximum of just over 50% early in February and then dropping to ~40% at the end of March, while the percentage differences between the single-layer simple chemistry integrations appeared to remain constant or increase slightly throughout the run (see E96, Figure 4a). Therefore this single figure of a 40% discrepancy does not give a full picture of either the SAOZ/3-D model comparison or the high-/low-resolution single-layer model comparison. More importantly, it must be emphasized that O_3 changes calculated at a single level (e.g., 450 K) cannot be quantitatively compared with column O_3 changes. Therefore the apparent quantitative agreement on a single number extracted from each of these two scenarios and its subsequent prominence in the arguments presented within E96 may be unjustified.

The results and conclusions of E96 raise questions about the the fidelity of results from all low-to-moderate resolution 3-D chemical transport model calculations, which in many respects appear to perform well [e.g., *Lefèvre et al.*, 1994; *Chipperfield et al.*, 1995], although there is evidence that such models underestimate polar O_3 loss [e.g., *Hansen et al.*, 1997]. Therefore the problems addressed by E96 need to be studied further. In this paper we have used a chemical transport model (CTM) to investigate further the effect of model resolution on polar O_3 loss, and we compare our results with those of E96. We have performed calculations for the Arctic winter of 1994-1995 using a range of model resolutions, advection schemes, and both a full and simplified chemistry scheme. First, we describe our CTM experiments and describe the two chemical schemes used. We then analyze the magnitude of ClO_x activation and O_3 depletion as a function of model resolution. We describe some sensitivity experiments to investigate the effect of assumptions in the simple chemistry scheme on the modeled loss. Finally, we discuss our results, which show little sensitivity to resolution, and contrast them to E96. In a companion paper [*Searle et al.*, this issue] we extend on these model runs and present a theoretical analysis of the expected sensitivity of polar O_3 loss to the distribution of ClO_x.

2. Model and Experiments

We have used the SLIMCAT off-line 3-D CTM, described in more detail by *Chipperfield et al.* [1996], to perform a range of single-level experiments on the 450 K isentropic surface. These model integrations were initialized on December 20, 1994, and integrated for 90 days until March 1995 using winds and temperatures from European Centre for Medium Range Weather Forecasts (ECMWF) analyses with a spectral resolution of T42. The CTM itself was run at the resolutions of a T21 Gaussian grid (5.6° × 5.6°), a T42 Gaussian grid (2.8° × 2.8°), and a T79 Gaussian grid (1.4° × 1.4°). The default model tracer advection scheme is the second-order moments scheme of *Prather* [1986] which has relatively low numerical diffusion. Other advection schemes are available in the model (e.g. a semi-Lagrangian scheme (see below)). We integrated the SLIMCAT CTM with two chemical schemes: a full chemistry scheme and a simple chemistry scheme based on that used by E96.

The full chemistry scheme contains the usual stratospheric O_x, NO_y, Cl_y, Br_y, and HO_x species and a treatment of heterogeneous chemistry on sulfate aerosols and polar stratospheric clouds (PSCs). The heterogeneous scheme is described by *Chipperfield et al.* [1993]; it does not contain any microphysics but calculates the equilibrium formation of nitric acid trihydrate (NAT) and ice particles on the basis of model temperature, H_2O field and HNO_3 field, and the surface area of liquid sulfate aerosol is advected as a passive tracer. The experiments described here contained no treatment of denitrification. The model used photochemical data from *DeMore et al.* [1994]. The full chemistry integrations were initialized using output from a two-dimensional (2-D) latitude-height model.

Our simple chemistry scheme is based as closely as possible on that used by E96. It considers only the ozone loss arising as a result of the ClO dimer cycle and treats two species: ozone and active chlorine (ClO_x = ClO + $2Cl_2O_2$). The chemical reactions considered are

$$\begin{aligned}
&\text{(R1)} && ClO + ClO + M &&\longrightarrow&& Cl_2O_2 + M\\
&\text{(R2)} && Cl_2O_2 + h\nu &&\longrightarrow&& 2Cl + O_2\\
&\text{(R3)} && Cl_2O_2 + M &&\longrightarrow&& ClO + ClO\\
&\text{(R4)} && Cl + O_3 &&\longrightarrow&& ClO + O_2
\end{aligned}$$

The partitioning of the ClO_x between ClO and its dimer is then given by

$$\frac{[Cl_2O_2]}{[ClO]} = \frac{k_1[ClO][M]}{J_2 + k_3[M]}$$

and the ozone loss rate equals $2J_2[Cl_2O_2]$, where J_2, k_1, and k_3 are the photolysis rate of Cl_2O_2, the rate constant of (R1), and the rate constant of (R3) respectively. There is no term for the production of ozone, but this will not be important in the wintertime polar lower stratosphere. Active chlorine is produced using a simple parameterization of PSC processing, with ClO_x being released at a constant rate ($RClO_x$ molecules cm^{-3} s^{-1}) within any grid box where the analysis temperature is 195 K or below. The default release rate was set to 6 molecules cm^{-3} s^{-1}. An upper limit of 3 parts per 10^9 by volume (ppbv) of ClO_x in any grid box is set to prevent the accumulation of unrealistic amounts. A chlorine sink is provided by reaction with NO_2 which is produced through the photolysis of HNO_3, present within the model at a constant background mixing ratio of 1 ppbv within PSC regions and 9 ppbv elsewhere. The scheme does not explicitly treat NO_2, rather the rate at which it is produced through photolysis is assumed to be equal to the rate at which ClO is destroyed. Thus NO_2 reacts as soon as it is produced and hence does not accumulate. The model does not consider the photolysis of $ClONO_2$, so once in the reservoir form, chlorine is removed from the model. The photolysis rates J come from the same look-up table as is used in the full chemistry scheme. To our knowledge these values (which are calculated from recommended cross sections) are the only quantitative difference between our simple chemistry scheme and that of E96.

The ozone depletion within each model grid box was determined from the difference between the chemically integrated ozone and the initial ozone field advected as a passive tracer. Mean vortical values for the mixing ratios of species and the percentage ozone depletion were obtained from a mass-weighted average of the fields inside the 25 PVU (1 PVU = 1×10^{-6} K m^2 kg^{-1} s^{-1}) contour.

3. Results

3.1. The Arctic Vortex

We performed six model integrations with resolutions from $5.6^o \times 5.6^o$ to $1.4^o \times 1.4^o$ with both the full and simple chemistry schemes. These experiments are summarized in Table 1 together with a summary of the results for the ozone depletion within the 25 PVU contour, suitable for comparison with E96.

3.1.1. Average ozone depletion. Figure 1 shows the average ozone depletion within the polar vortex for the six experiments listed in Table 1. The two main features of Figure 1 are the small effect of resolution on the calculated ozone loss and the much larger loss calculated with the simple scheme by the end of the winter.

The final ozone depletion shown in Figure 1 is plotted in Figure 2 as a function of model grid resolution. Figure 2 also shows the maximum local loss in any grid box within the polar vortex over the same period. The small resolution dependence of the SLIMCAT results can again be seen. Figure 2 also shows results from E96 (estimated from their figures). For the resolutions used in E96 they obtain a much larger variation with resolution with much lower depletion at low resolution.

3.1.2. Ozone depletion and ClO_x. There are clearly major differences between the results shown in Table 1 and those in E96. A comparison of the SLIMCAT simple chemistry scheme's performance with the results from E96 shows that SLIMCAT not only produces much more seasonal ozone loss within the vortex but also has less sensitivity to model resolution. Looking at the full chemistry examples in Table 1, there is no trend in ozone loss with resolution, and the maximum difference between the three cases is $< 2\%$ over 90 days.

The difference in ozone loss calculated with the simple and full chemistry schemes (Figure 2) is due to different levels of active chlorine (ClO_x). The vortex average ClO_x for experiments F79 and S79 is shown in Figure 3 and is also apparent from the plots of ClO_x fields for February 14 (in Plate 1 below). The simple chemistry scheme processes more chlorine into active forms than the full chemistry scheme; in fact, for a large proportion of January and February the vortex in the simple scheme is very nearly fully activated, and the ClO_x values in some grid boxes are limited by the imposed 3 ppbv maximum. The shallower ClO_x decay gradient in the simple scheme indicates that relative to the full

Table 1. SLIMCAT Integrations at Different Resolutions

Run	Grid Resolution		Chemistry	Percent Depletion[a]	Maximum Percent Depletion[b]
	Degrees	Kilometers	Scheme	March 20, 1995	1994-1995 Winter
F79	1.4 x 1.4	~80	full	32.7	49.5
F42	2.8 x 2.8	~150	full	32.0	46.6
F21	5.6 x 5.6	~300	full	33.7	48.7
S79	1.4 x 1.4	~80	simple	61.3	85.7
S42	2.8 x 2.8	~150	simple	58.7	77.6
S21	5.6 x 5.6	~300	simple	55.7	72.5

[a] Percent depletion is the average within the 25 PVU contour; 1 PVU = 1×10^{-6} K m^2 kg^{-1} s^{-1}.

[b] Maximum percent depletion is the largest loss produced in any individual grid box throughout the duration of the integrations.

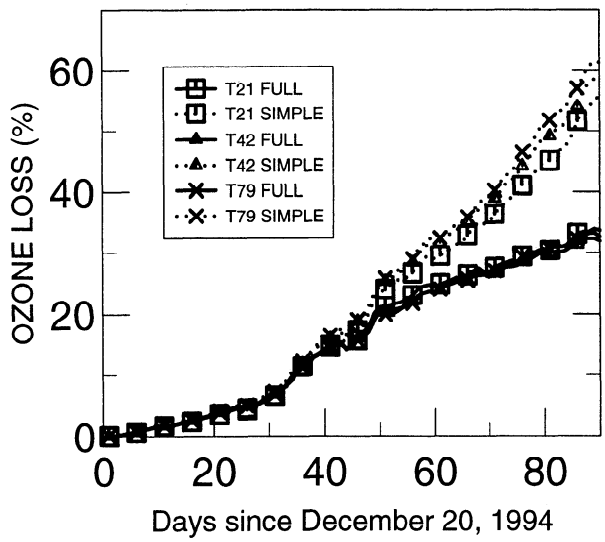

Figure 1. Accumulated ozone depletion (%) averaged within the 25 PVU contour from the SLIMCAT model at different resolutions for both the full and simple chemical schemes. 1 PVU = 1×10^{-6} K m^2 kg^{-1} s^{-1}.

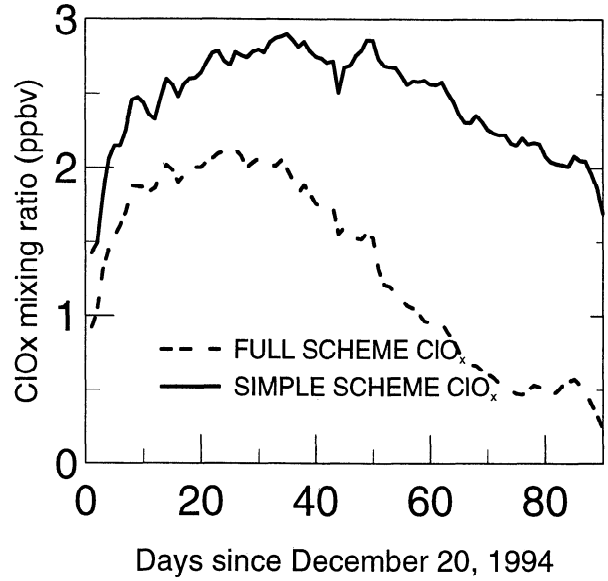

Figure 3. Mean ClO_x mixing ratios within the Arctic vortex (25 PVU contour) for SLIMCAT integrations F79 and S79. In the simple chemistry scheme the ClO_x mixing ratio in any box is limited to 3 ppbv.

chemical scheme, deactivation is taking place too slowly. Figure 4 shows the ClO_x in the remnants of the vortex on the last day of the 90 day run (March 20, 1995). In the simple scheme the vortex, though small, is still strongly activated.

3.1.3. Time evolution of the O_3 loss. Although Figure 1 appears to show that the ozone loss curves for the two schemes match well until about day 50 of the run, closer inspection shows that particularly at the higher resolutions, the curves diverge from around day 30. From Figure 5 we can see that at day 30 the concentration of $ClONO_2$ in the full chemistry scheme starts to increase and the total HNO_3 (solid + gas phase) and ClO_x decrease. $ClONO_2$ is formed by

$$ClO + NO_2 + M \longrightarrow ClONO_2 + M$$

The NO_2 is formed through the photolysis of HNO_3,

$$\text{(R5)} \qquad HNO_3 + h\nu \longrightarrow NO_2 + OH$$

and through its reaction with OH,

$$\text{(R6)} \qquad OH + HNO_3 \longrightarrow H_2O + NO_3$$

The NO_3 formed in this reaction is rapidly converted to NO_2, and since OH radicals are produced predominantly through photolysis, both reactions will have a rate which is strongly dependent on the amount of sunlight present. They both contribute to chlorine deactivation in the Arctic polar vortex [*Chipperfield et al.*, 1997]. The small quantities of $ClONO_2$ produced for the first 30 days of the integration thus indicate that the vortex is mainly in darkness during this period. Substantial removal of ClO_x and HNO_3 together with the production of $ClONO_2$ after day 30 indicate the presence of significant levels of sunlight. Photolysis of Cl_2O_2 in the dimer cycle means that ozone depletion also depends on the amount of sunlight; therefore during the initial stages of the integration, darkness within the vortex prevents substantial depletion from occurring.

Figure 6 shows the position of the vortex on days 25, 29, 33, and 37 of the integration. Around this time a strong minor warming occurred in the upper stratosphere and moved the center of the vortex in the lower

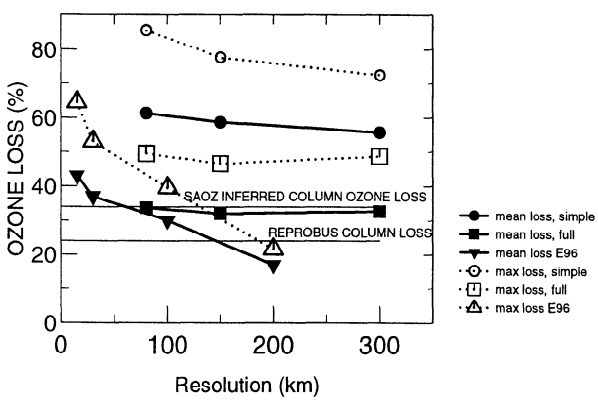

Figure 2. Average percent ozone loss over the 1994-1995 northern hemisphere (NH) winter within the 25 PVU contour and the peak percentage loss within a grid box within the same region and over the same period as a function of model resolution for the simple and full chemical schemes. Also shown are the model results from E96 and their estimates of O_3 loss derived from observations (SAOZ) and from a full 3-D model (REPROBUS).

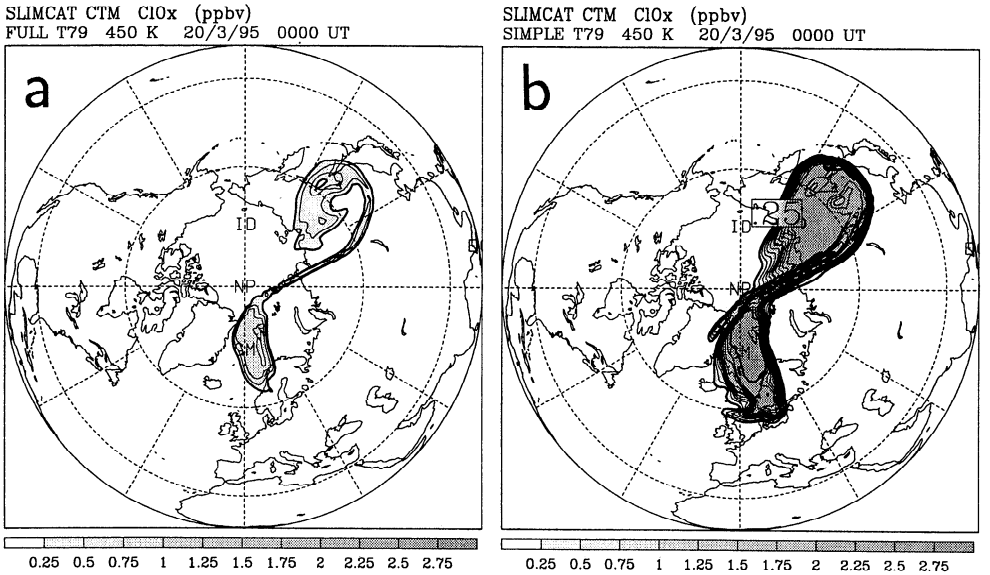

Figure 4. Distribution of ClO_x (ppbv) on March 20, 1995, from (a) run F79 and (b) run S79.

stratosphere off the pole, thus exposing more of the activated air to sunlight and bringing a marked increase in the rate of ozone depletion. The effects of this movement of the vortex explain the changes in mixing ratio of major species, noted from Figure 5, which take place at this time. The increase in levels of sunlight within the 25 PVU contour also explains the divergence of the two chemistry schemes because the very large mean mixing ratios of ClO_x in the simple chemistry scheme allow it to destroy ozone more quickly than the full chemistry scheme.

The larger amounts of ClO_x in the simple scheme arise both as a result of too much production and too little deactivation. The fact that levels of active chlorine in the simple scheme rise so quickly at the start of the integration, compared with levels in the full scheme (Figure 3) suggests that the rate of chlorine release from the simple PSC parameterization is overestimated. Fig-

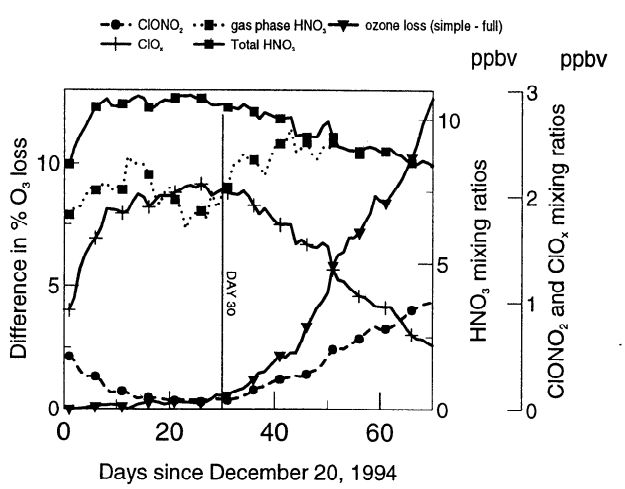

Figure 5. Evolution of ClO_x, $ClONO_2$, and both condensed and gas phase HNO_3 for the first 70 days of the integration F79 together with the difference in percent ozone destroyed between the full and simple chemistry schemes. The vertical line at day 30 marks the time when the ozone losses from the two schemes start to diverge. This coincides with the increase in $ClONO_2$.

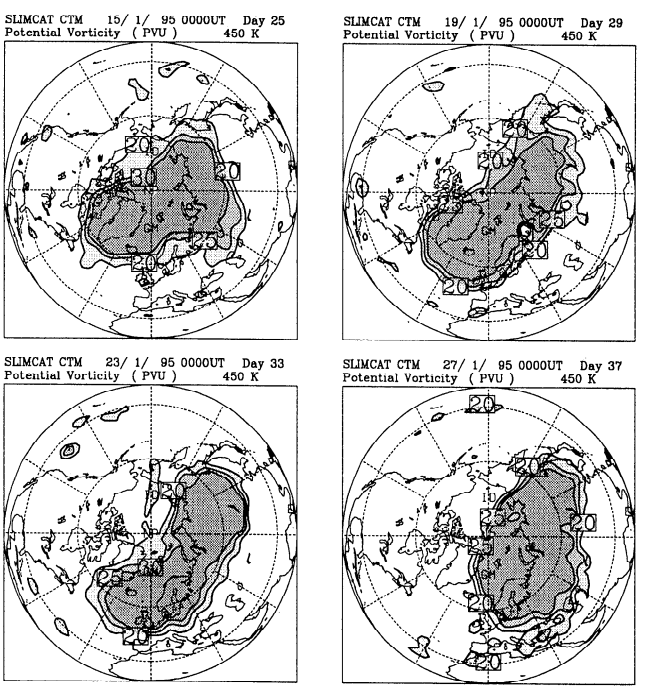

Figure 6. Evolution of the 20, 25, and 30 PVU contours on the 450 K surface during mid-January 1995. At this time the vortex was disturbed by a strong minor warming at higher levels. This pushes the vortex off the pole and into sunlight, causing the acceleration in the rate of ozone depletion evident in the model runs at this time.

ure 7 shows that for much of the integration, gas phase HNO_3 in the full chemistry run is higher than in the simple chemistry run. In addition, the simple chemistry scheme neglects (R6), which can be as important as the HNO_3 photolysis in chlorine deactivation at the vortex edge [*Chipperfield et al.*, 1997]. Therefore the rate of NO_2 release, and the rate at which ClO is sequestered into $ClONO_2$, will be underestimated in the simple scheme. Figure 7 can also be used to view where temperatures in the vortex fall below the PSC threshold temperature: a value for the average HNO_3 mixing ratio in the simple scheme of exactly 9 ppbv indicates that there are no PSCs. It confirms that temperatures rose above the PSC threshold throughout the vortex in late February before falling once again, permitting renewed activation, at the beginning of March.

3.1.4. ClO_x fields. Plate 1 shows the ClO_x fields from the six SLIMCAT runs on February 14, 1995. At this time the vortex is in the throes of a major disturbance in which it has split into two centers: the major one centered over the pole and the minor one over east Asia, north of Japan. The smaller part is in the process of being mixed into middle latitudes.

Comparing first the results from the two different chemistry schemes, we can see that the simple scheme leads to very much larger amounts of chlorine: typical mixing ratios within the simple chemistry case are above 2.75 ppbv, while those in the full scheme are on average ~1 ppbv lower, with typical values between 1.5 and 2 ppbv. The larger vortex center values of ClO_x in the simple case lead to a southerly extension of the area containing significant quantities of active chlorine and also permits filamentary ClO_x structures which form in midlatitudes to persist for longer. Hence, whereas the filament connecting the two vortex centers has vanished in the full chemical integrations, even at the highest resolution, this feature is still present in the simple chemistry runs, even at low resolution ($5.6^o \times 5.6^o$). This suggests that the more rapid disappearance of filamentary ClO_x structures at low resolution, by comparison to high-resolution runs, stems not only from the greater numerical diffusion (causing the feature to be mixed in more quickly), but also from the ClO_x within the filaments reacting away more quickly. These two effects will tend to enhance each other. On a more general level these results also suggest that the lifetime of a filament of a relatively reactive species will depend not only on the dynamical mixing but also on the chemistry of the species and the impact of mixing on its chemistry.

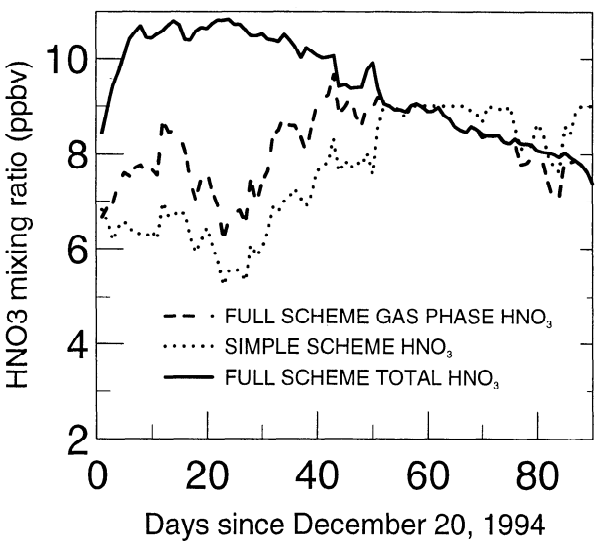

Figure 7. Mean values of the total and gas phase HNO_3 within the 25 PVU contour from run F79 and HNO_3 from run S79. When there are no temperatures below 195 K, the HNO_3 mixing ratio from the simple scheme equals the 9 ppbv vortex background value.

We now discuss the effects of resolution on the structures present within the model fields. We see more structure within the high-resolution fields, though no new features appear; this greater structure leads to a wider range of mixing ratio values, with higher maxima (not always possible in the simple chemistry scheme because of the 3 ppbv ceiling placed on ClO_x mixing ratios), lower minima, and sharper gradients in between. Note, however, that although more structure exists within the vortex at higher resolutions, this region is not filled with grid-scale-length features. On the contrary, it is fairly uniform and, owing to limited shear and strain in the wind field of this region, features here are as likely to have been introduced through slight differences in the area exposed to low temperature as through significant differences in the amounts of mixing produced by the advection scheme.

3.1.5. Comparison with Microwave Limb Sounder ClO data. For the winter 1994-1995, satellite observations of ClO in the lower stratosphere are available on certain days from the Microwave Limb Sounder (MLS) [*Manney et al.* 1996]. Given the large differences observed in the ClO_x fields of the simple and and full chemistry schemes in our model runs, and between our model runs and those of E96, the MLS ClO data can be used to indicate qualitatively which simulations are most realistic.

Figure 8 shows the ClO fields from the S79 and F79 integrations on the February 3 and 14. In the full chemistry case the ClO values on February 3, during the period of maximum activation, are between 0.9 and 1.8 ppbv in the vortex center. In the simple chemistry scheme the ClO values are in the range 1.35-2.25 ppbv. The plots of MLS ClO in Plate 2 indicate that ClO mixing ratios are of a similar magnitude to those calculated by the full chemical scheme. This demonstrates that the vortex in the simple scheme runs is overactivated.

On the February 14, a period when higher temperatures have stopped ClO_x activation, the full chemistry scheme run shows values of <1 ppbv of ClO within the vortex, whereas the simple scheme run indicates values between 0.9 and 1.8 ppbv. MLS data again indicate values which are in accordance with those from the full scheme.

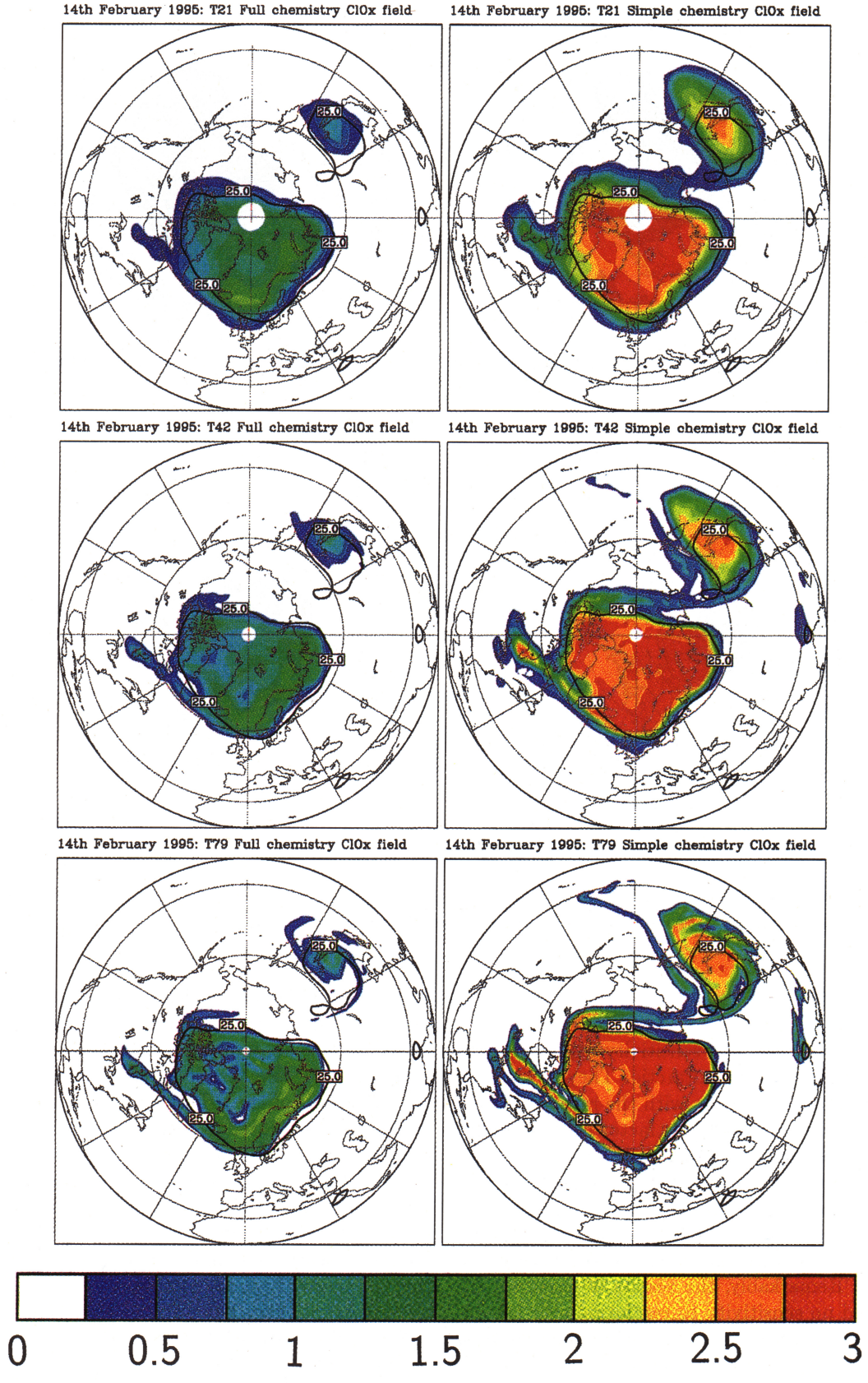

Plate 1. Model ClOx distribution on February 14 at the three resolutions using the full and simple chemistry schemes.

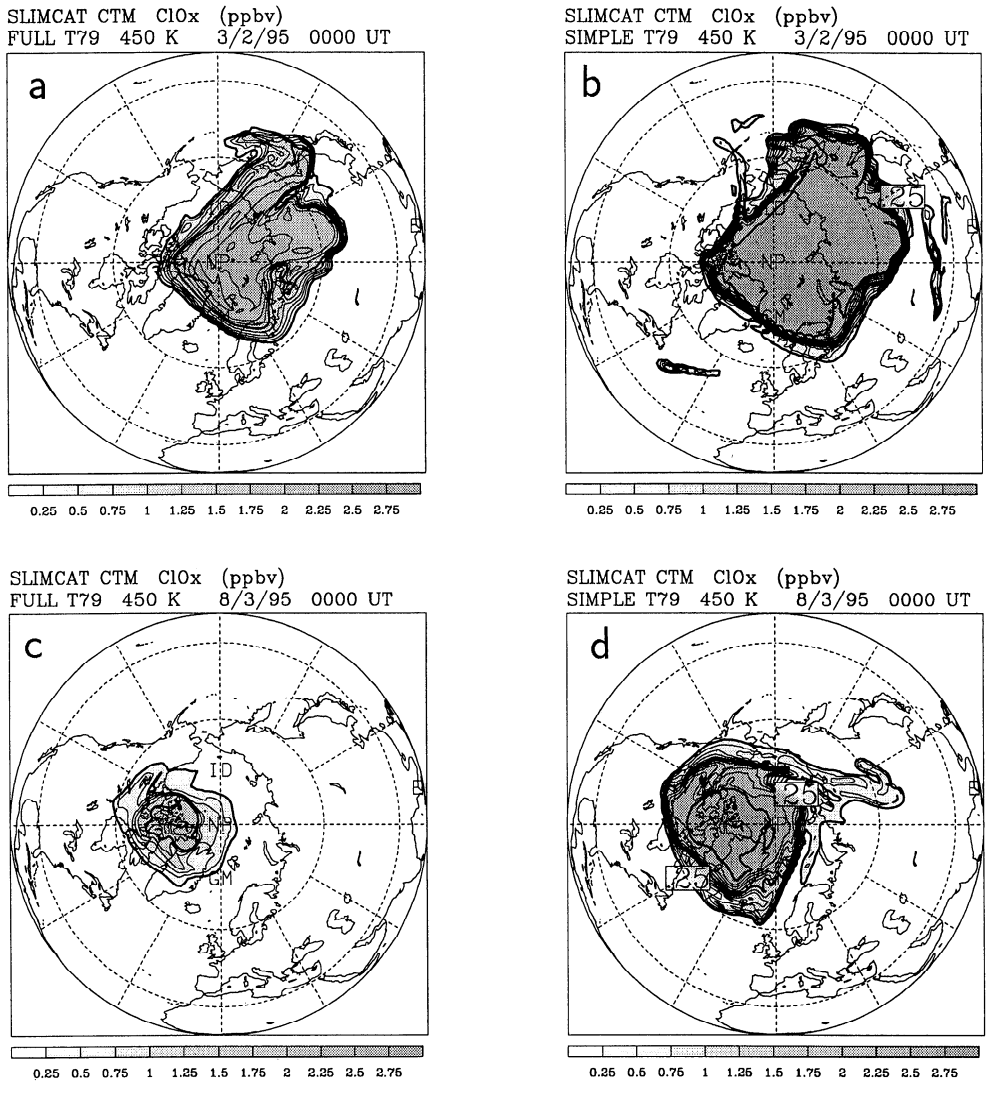

Figure 8. ClO_x from the simple and full chemistry integrations (b) and (d) S79 and (a) and (c) F79 for February 3 (Figures 8a and 8b) and March 8 (Figures 8c and 8d).

3.2. The "Antarctic" Case

E96 performed a range of sensitivity experiments to simulate conditions in the Antarctic. They did this by running the Arctic case study with the rate of chlorine release from PSCs increased by a factor of 10 over that used in the previous case (to 60 molecules cm^{-3} s^{-1}). This was done to account for the greater amounts of chlorine activation produced by the lower temperatures which would be seen in the Antarctic analyses and also the greater denitrification in the southern hemisphere (SH). Remarkably, the results of these experiments showed no sensitivity to resolution over the 15-200 km range of grid boxes sizes, in marked contrast to their Arctic case. E96 also calculated a model ozone loss of more than 95% by day 55 of the run. This, in effect, suggests that if the E96 integrations were somewhat representative of the Antarctic winter conditions, ozone depletion in the Antarctic should reach 95% loss by the end of August, which is not consistent with observations; O_3 losses reaching these levels are only observed by late September.

Given the parameters of the simple chemistry scheme, the conditions of the SH winter would have been more realistically simulated by altering quantities such as the temperature (i.e., reducing it to form PSCs over a larger area and for longer periods as observed in the Antarctic) or the denitrification (in this case, reducing the background of HNO_3 from 9 ppbv). These changes would have been more meaningful than the rate at which chlorine is released from the surfaces of PSCs which should not necessarily vary between the hemispheres.

For further comparison with the results of E96 we ran the SLIMCAT model with a variety of chlorine release rates in the simple chemistry scheme as well as a case where the concentrations of ClO_x were maintained at the 3 ppbv limit throughout the run. The results from these runs are listed and detailed in Table 2 and may

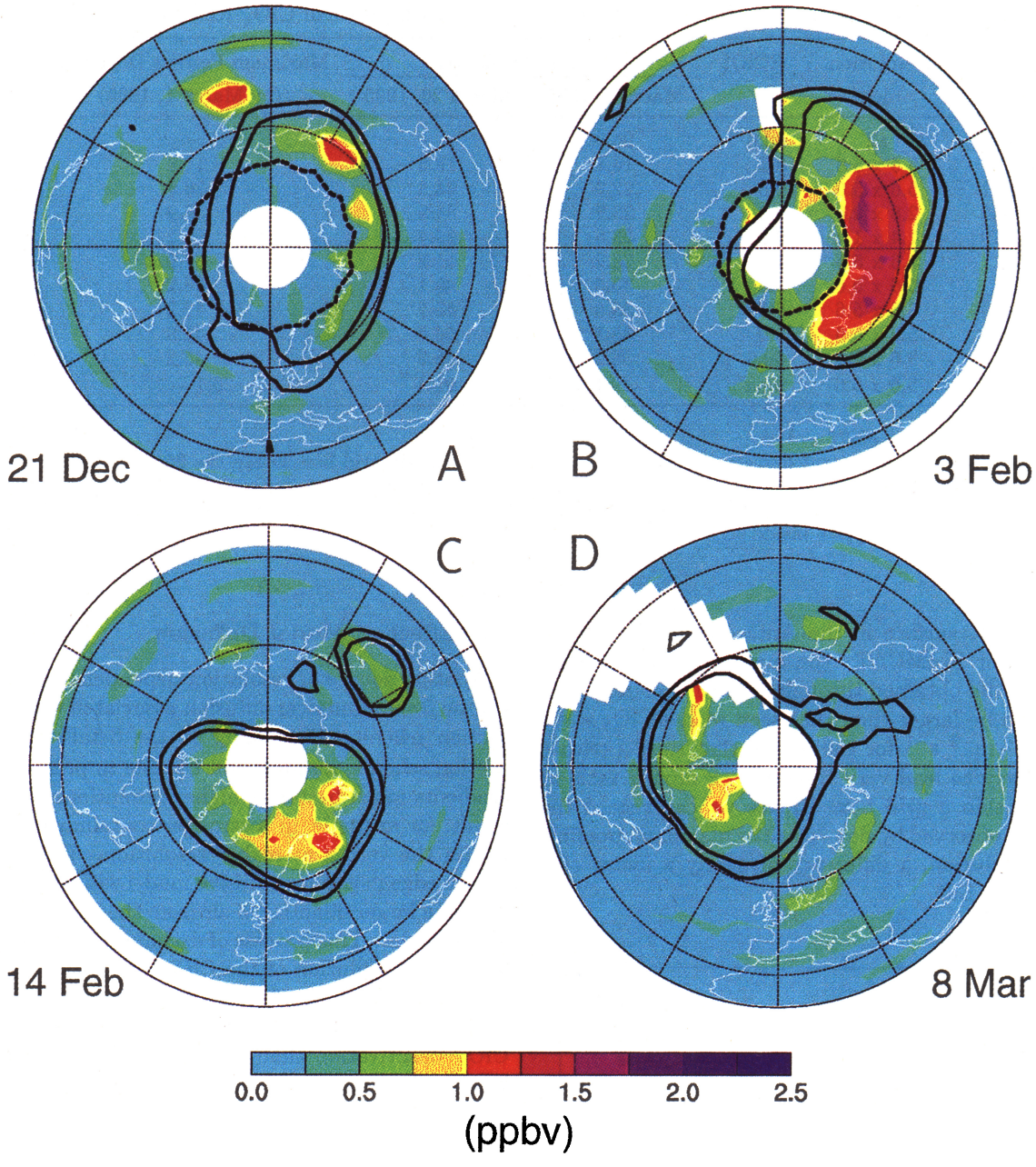

Plate 2. Microwave Limb Sounder (MLS) version 4 observations of ClO on the 465 K isentropic surface for the northern hemisphere for (a) December 21, 1994, (b) February 3, 1995, (c) February 14, 1995 and (d) March 8, 1995. The black lines are the 25 and 30 PVU contours, and the dotted black line in Plates 2a and 2b is the 94° solar zenith angle contour. Blank spaces indicate missing data or poor retrieval quality. Data are courtesy of M.L. Santee.

be compared with figures for the northern hemisphere (NH) loss in Table 1.

Figure 9 shows the expected increase in ozone loss with increasing $R\mathrm{ClO}_x$. At low values of $R\mathrm{ClO}_x$ the loss is sensitive to the release rate, but as it is increased, the sensitivity diminishes dramatically, with just a 1% change in the amount of loss for a tenfold increase in the release rate of ClO_x from 6 to 60. This may be understood as a saturation effect caused by the 3 ppbv upper limit on ClO_x preventing the larger rates of release from having any effect.

Regarding the magnitude of O_3 loss, our results are again inconsistent with those of E96. Their figure of 95% loss by the first of March in the Antarctic case is nearly twice the size of the loss observed with SLIMCAT when the ClO_x mixing ratio is set to 3 ppbv throughout the whole winter, and as previously mentioned, it also suggests that there could be almost complete ozone loss

Table 2. Summary of SLIMCAT Integrations With Varying Rate of ClO_x Release

Run	Resolution, deg	$RClO_x^a$	Percent Depletion		Maximum Percent Depletion[b] (by March 1, 1995)
			March 1, 1995	March 20, 1995	
E96[c]	all	60.0	95.0	—	—
a	5.6 x 5.6	0.1	10.3	13.5	17.3
b21	5.6 x 5.6	0.5	22.0	34.3	30.8
b42	2.8 x 2.8	0.5	23.2	34.5	36.9
b79	1.4 x 1.4	0.5	23.6	35.4	51.1
c	5.6 x 5.6	1.0	26.2	41.8	32.9
d	5.6 x 5.6	2.0	30.5	49.1	38.2
e	5.6 x 5.6	6.0	35.0	55.7	42.2
f	5.6 x 5.6	9.0	35.7	56.8	42.8
g	5.6 x 5.6	60.0	36.2	58.2	43.2
h	5.6 x 5.6	max[d]	49.1	91.4	20.1

[a] molecules cm^{-3} s^{-1}.
[b] Maximum percent depletion is the largest % loss seen in any grid box within the 25 PVU contour up to March 1, 1995.
[c] Run E96 shows our analysis of the results from the E96 Antarctic integrations at all resolutions.
[d] $[ClO_x]$ = 3 ppbv inside 25 PVU at all times.

on the 450 K surface in the Antarctic by the end of August. For SLIMCAT the maximum possible loss which may be obtained through alteration of $RClO_x$ is unlikely to be larger than that seen with $RClO_x$ = 60 molecules cm^{-3} s^{-1} for the reason that such a release rate is likely to lead very rapidly to a mixing ratio of 3 ppbv within a grid box. Hence we can regard the 36.2% loss observed by day 70 as the maximum possible at this resolution, a difference of nearly a factor of 3 compared to E96.

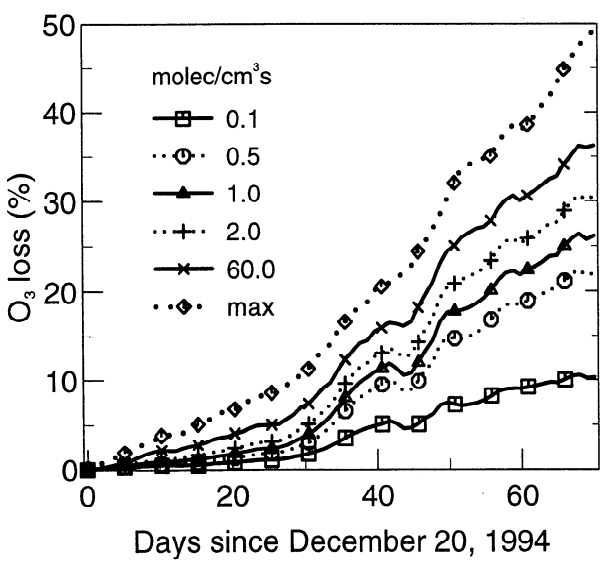

Figure 9. Ozone loss (%) within the 25 PVU contour from the SLIMCAT simple chemistry scheme at 5.6° × 5.6° for different values for the release rate of active chlorine from polar stratospheric clouds (PSCs). In the experiment labeled "max" the ClO_x mixing ratio was set to 3 ppbv throughout the run within the 25 PVU contour.

3.3. Effect of Model Diffusion

Another source of resolution dependency in a model will be from numerical diffusion associated with the advection scheme. Depending on the details of the advection scheme, a model will be able to preserve sharp gradients much better at higher resolutions. This may result, for example, in a stronger containment of ClO_x within the vortex at higher resolution. Therefore the vortex edge in a more diffusive model will allow the passage of a larger quantity of air from the vortex into middle latitudes. This process of exchange will be two-way, leading to a dilution of the ClO_x and a dilution of the ozone-depleted air. *Thuburn and Tan* [1997] showed, using a model with a more detailed treatment of the ClO_x deactivation than our simple scheme, that this increased mixing of activated and nonactivated air led to an increased rate of reaction of ClO with NO_2.

We performed a series of integrations run using two different advection schemes: the default *Prather* [1986] scheme and a more diffusive semi-Lagrangian scheme [*Williamson and Rasch*, 1989]. By comparing these results (not shown) with those in Table 1 we find a stronger dependency of the polar ozone loss with advection scheme (i.e., numerical diffusion) than with resolution; the more diffusive the advection scheme, the smaller the ozone loss. For example, the amount of ozone loss produced by our most diffusive advection scheme, the flux-limited semi-Lagrangian scheme, at 1.4° × 1.4° resolution (grid box size of ~80 km) is 53.3% compared with 61.3% with the default *Prather* [1986] scheme. However, this change is still small relative to the changes found by E96; for a similar resolution, E96 find an ~30% loss. It may be that the E96 model is more diffusive than our model; however we are not in a position to confirm this.

4. Discussion

The results outlined above indicate major differences between the behavior of our SLIMCAT model and the model used by E96. These differences can be summarized as follows:

1. E96 find that the calculated polar O_3 loss is very sensitive to the resolution at which their model is run, whereas SLIMCAT shows little sensitivity with the simple chemical scheme and even less when run with the full chemistry scheme.

2. In the case of a simplified ClO_x–only chemistry scheme a comparison of the amounts of ozone depletion obtained shows that for a chlorine release rate of 6 molecules cm^{-3} s^{-1}, there is 61% depletion in the highest-resolution SLIMCAT integration, and only 43% in the highest-resolution E96 integration.

3. When the rate of chlorine release is increased to 60 molecules cm^{-3} s^{-1}in the "Antarctic" case, we find that SLIMCAT produces only about half the depletion seen in E96. In fact, even when the ClO_x mixing ratio is set to its maximum value of 3 ppbv throughout the winter, SLIMCAT is unable to reproduce the very large losses which E96 calculate.

4. We find a stronger dependency of ozone depletion on the diffusiveness of the model advection scheme than on resolution. However, even a relatively diffusive semi-Lagrangian scheme still produces more ozone depletion than the calculations of E96 at a similar resolution.

5. Summary and Conclusions

We have used an off-line chemical transport model to investigate the effect of model resolution on the calculated ozone depletion within the Arctic polar vortex. One motivation for our study is the recent work of *Edouard et al.* [1996] (E96), who found a very strong dependence of ozone loss due to the ClO-ClO cycle in their model, which they attributed to the effect of averaging small-scale features

Our integrations with the SLIMCAT model using both a full stratospheric chemistry scheme and a simplified ClO_x–only scheme, based on that used by E96, display only a small resolution dependence. This lack of sensitivity is due to the effectively complete activation of chlorine at all model resolutions during this cold winter, which removes any potential effect of spatial averaging on the ClO distribution. The small changes we do see with the simple scheme are consistent with small changes in the levels of cross-vortex-edge diffusion giving less ClO_x in the vortex at low resolution. The full stratospheric chemistry scheme exhibits no systematic changes in ozone loss with resolution, and the range of results for O_3 loss over the season is very small.

Further integrations performed using two advection schemes with different numerical diffusion suggest that the amount of polar ozone loss in the model is more sensitive to changes in the diffusiveness of the advection scheme, although the effect is still relatively small.

From studying the model chemical fields we note that the types of filamentary structures produced by the model are affected by the chemistry scheme employed. Narrow filaments, which are no longer apparent in the full chemistry integrations, persist for much longer in the simple chemistry case at the same resolution. This suggests that chemistry, as well as dynamics, is extremely important in determining the lifetimes of filamentary features of some reactive species present in some fields.

Acknowledgments. We thank S. Edouard and B. Legras for supplying further details of their study. We are grateful to J. Waters and M. L. Santee for supplying the MLS ClO data. KRS thanks NERC for a studentship; MPC thanks NERC for an Advanced Fellowship. This work forms part of the NERC UGAMP programme and was supported by the CEC through contract ENV4-CT95-0050. We thank the reviewers for their comments.

References

Chipperfield, M.P., D. Cariolle, P. Simon, R. Ramaroson and D.J. Lary, A three-dimensional modeling study of trace species in the Arctic lower stratosphere during winter 1989-1990, *J. Geophys. Res.*, *98*, 7199-7218, 1993.

Chipperfield, M.P., J.A. Pyle, C.E. Blom, N. Glatthor, M. Höpfner, T. Gulde, C. Piesch, and P. Simon, The variability of $ClONO_2$ and HNO_3 in the Arctic polar vortex: Comparison of Transall Michelson interferometer for passive atmospheric sounding measurements and three-dimensional model results, *J. Geophys. Res.*, *100*, 9115-9129, 1995.

Chipperfield, M.P., M.L. Santee, L. Froidevaux, G.L. Manney, W.G. Read, J.W. Waters, A.E. Roche, and J.M. Russell, Analysis of UARS data in the southern polar vortex in September 1992 using a chemical transport model, *J. Geophys. Res.*, *101*, 18,861-18,881, 1996.

Chipperfield, M.P., E.R. Lutman, J.A. Kettleborough, J.A. Pyle, and A.E. Roche, Model studies of chlorine deactivation and formation of $ClONO_2$ collar in the Arctic polar vortex, *J. Geophys. Res.*, *102*, 1467-1478, 1997.

DeMore, W.B., S.P. Sander, D.M. Golden, R.F. Hampson, M.J. Kurylo, C.J. Howard, A.R. Ravishankara, C.E. Kolb, and M.J. Molina, Chemical kinetics and photochemical data for use in stratospheric modeling: Evaluation no. 11, JPL Publ. *94-26*, pp 273, 1994.

Edouard, S., B. Legras, F. Lefèvre, and R. Eymard, The effect of small-scale inhomogeneities on ozone depletion in the Arctic, *Nature*, *384*, 444-447, 1996.

Goutail, F., et al., Total ozone depletion in the Arctic during the winters of 1993-94 and 1994-95, *J. Atmos. Chem.* in press, 1998.

Hansen, G., T. Svenoe, M.P. Chipperfield, A. Dahlback and U.P. Hoppe, Evidence of substantial ozone depletion in winter 1995/96 over northern Norway, *Geophys. Res. Lett.*, *24*, 799-802, 1997.

Kaye, J.A., Analysis of the effects of zonal averaging on rate of reaction calculations in two-dimensional atmospheric models, *J. Geophys. Res.*, *92*, 11,965-11,970, 1987.

Lefèvre, F., G.P. Brasseur, I. Folkins, A.K. Smith, and P. Simon, Chemistry of the 1991-1992 stratospheric winter:

Three-dimensional model simulations, *J. Geophys. Res.*, *99*, 8183-8195, 1994.

Manney, G.L., L. Froidevaux, J.W. Waters, M.L. Santee, W.G. Read, D.A. Flowers, R.F. Jarnot, and R.W. Zurek, Arctic ozone depletion observed by UARS MLS during the 1994-95 winter, *Geophys. Res. Lett.*, *23*, 85-88, 1996.

Prather, M.J., Numerical advection by conservation of second-order moments, *J. Geophys. Res.*, *91*, 6671-6681, 1986.

Pyle, J.A., and A.M. Zavody, The modelling problems associated with spatial averaging, *Q. J. R. Meteorol. Soc.*, *116*, 753-766, 1990.

Searle, K.R., M.P. Chipperfield, S. Bekki, and J.A. Pyle, The impact of spatial averaging on calculated polar ozone loss, 2, Theoretical analysis, *J. Geophys. Res.*, this issue.

Tan, D.G.H., P.H. Haynes, A.R. MacKenzie, and J.A. Pyle, The effects of fluid dynamical stirring and mixing on the deactivation of stratospheric chlorine, *J. Geophys. Res.*, *103*, 1585-1605, 1998.

Thuburn, J., and D.G.H. Tan, A parameterization of mixdown time for atmospheric chemicals, *J. Geophys. Res.*, *102*, 13,037-13,049, 1997.

Tuck, A.F., A comparison of one-, two-, and three-dimensional model representations of stratospheric gases, *Philos. Trans. R. Soc. London, Ser. A*, *290*, 477-494, 1979.

Williamson, D.L., and P.J. Rasch, Two-dimensional semi-Lagrangian transport with shape preserving interpolation, *Mon. Weather Rev.*, *117*, 102-129, 1989.

S. Bekki, Service d'Aeronomie du Centre National de la Recherche Scientifique, Université Pierre et Marie Curie, 4 Place Jussieu, 75230 Paris Cedex 05, France. (e-mail: slimane@aero.jussieu.fr)

M.P. Chipperfield and J.A. Pyle, Department of Chemistry, Cambridge University, Lensfield Road, Cambridge CB2 1EW, England, U.K. (e-mail: martyn@atm.ch.cam.ac.uk; pyle@atm.ch.cam.ac.uk)

K.R. Searle, United Kingdom Meteorological Office, London Road, Bracknell RG12 2SZ, England, U.K. (e-mail: krward@meto.gov.uk)

(Received February 27, 1998; revised June 5, 1998; accepted June 16, 1998.)